Analysis of genetic diversity and population structure of *Magnaporthe grisea*, the causal agent of foxtail millet blast using microsatellites (#83012)

First submission

Guidance from your Editor

Please submit by **13 Apr 2023** for the benefit of the authors (and your token reward) .

Structure and Criteria
Please read the 'Structure and Criteria' page for general guidance.

Raw data check
Review the raw data.

Image check
Check that figures and images have not been inappropriately manipulated.

If this article is published your review will be made public. You can choose whether to sign your review. If uploading a PDF please remove any identifiable information (if you want to remain anonymous).

Files

Download and review all files from the materials page.

7 Figure file(s)
4 Table file(s)
1 Raw data file(s)
2 Other file(s)

Structure and Criteria

Structure your review

The review form is divided into 5 sections. Please consider these when composing your review:

1. **BASIC REPORTING**
2. **EXPERIMENTAL DESIGN**
3. **VALIDITY OF THE FINDINGS**
4. General comments
5. Confidential notes to the editor

📄 You can also annotate this PDF and upload it as part of your review

When ready [submit online](#).

Editorial Criteria

Use these criteria points to structure your review. The full detailed editorial criteria is on your [guidance page](#).

BASIC REPORTING

- Clear, unambiguous, professional English language used throughout.
- Intro & background to show context. Literature well referenced & relevant.
- Structure conforms to [PeerJ standards](#), discipline norm, or improved for clarity.
- Figures are relevant, high quality, well labelled & described.
- Raw data supplied (see [PeerJ policy](#)).

EXPERIMENTAL DESIGN

- Original primary research within [Scope of the journal](#).
- Research question well defined, relevant & meaningful. It is stated how the research fills an identified knowledge gap.
- Rigorous investigation performed to a high technical & ethical standard.
- Methods described with sufficient detail & information to replicate.

VALIDITY OF THE FINDINGS

- *ⓘ* Impact and novelty not assessed. *Meaningful* replication encouraged where rationale & benefit to literature is clearly stated.
- All underlying data have been provided; they are robust, statistically sound, & controlled.

- Conclusions are well stated, linked to original research question & limited to supporting results.

Standout reviewing tips

The best reviewers use these techniques

Tip	Example
Support criticisms with evidence from the text or from other sources	*Smith et al (J of Methodology, 2005, V3, pp 123) have shown that the analysis you use in Lines 241-250 is not the most appropriate for this situation. Please explain why you used this method.*
Give specific suggestions on how to improve the manuscript	*Your introduction needs more detail. I suggest that you improve the description at lines 57- 86 to provide more justification for your study (specifically, you should expand upon the knowledge gap being filled).*
Comment on language and grammar issues	*The English language should be improved to ensure that an international audience can clearly understand your text. Some examples where the language could be improved include lines 23, 77, 121, 128 – the current phrasing makes comprehension difficult. I suggest you have a colleague who is proficient in English and familiar with the subject matter review your manuscript, or contact a professional editing service.*
Organize by importance of the issues, and number your points	*1. Your most important issue* *2. The next most important item* *3. ...* *4. The least important points*
Please provide constructive criticism, and avoid personal opinions	*I thank you for providing the raw data, however your supplemental files need more descriptive metadata identifiers to be useful to future readers. Although your results are compelling, the data analysis should be improved in the following ways: AA, BB, CC*
Comment on strengths (as well as weaknesses) of the manuscript	*I commend the authors for their extensive data set, compiled over many years of detailed fieldwork. In addition, the manuscript is clearly written in professional, unambiguous language. If there is a weakness, it is in the statistical analysis (as I have noted above) which should be improved upon before Acceptance.*

Analysis of genetic diversity and population structure of *Magnaporthe grisea*, the causal agent of foxtail millet blast using microsatellites

Manimozhi Dhivya [1] , **Govindasamy Senthilraja** [Corresp., 2] , **Nagendran Tharmalingam** [Corresp., 3] , **Sankarasubramanian Harish** [2] , **Kalaiselvan Saravanakumari** [2] , **Theerthagiri Anand** [2] , **Sundararajan Thiruvudainambi** [1]

[1] Department of Pathology, Agricultural College and Research Institute, Tamilnadu Agricultural university, Madurai 625104, Tamilnadu, India

[2] Department of Plant Pathology, Tamil Nadu Agricultural University, Coimbatore 641003, Tamilnadu, India

[3] Infectious disease/ Medicine, The Miriam Hospital/ Rhode Island Hospital, Brown University, Providence, RI, United States

Corresponding Authors: Govindasamy Senthilraja, Nagendran Tharmalingam
Email address: senthilraja@tnau.ac.in, nagendran_tharmaligam@brown.edu

Foxtail millet blast caused by *Magnaporthe grisea* is becoming a severe problem of foxtail millet farming in all over-regions of India. Information on the genetic diversity and population structure of foxtail millet infecting *M. grisea* is essential for developing effective management strategies, including the breeding of blast-resistant cultivars. We analysed thirty-two *M. grisea* isolates from ten foxtail millet growing districts in Tamil Nadu, India for genetic diversity using twenty-nine microsatellite or Simple Sequence Repeat (SSR) markers in this study. A total of 103 alleles were identified, with a mean of 3.55 alleles/locus. Gene diversity ranged from 0.170 to 0.717, while major allelic frequencies ranged from 0.344 to 0.906. The polymorphism information content (PIC) value was identified as 0.155 to 0.680, with an average value of 0.465. Population structure analysis of genomic data sets revealed two major populations (SP1 and SP2) with different levels of ancestral admixture among the 32 blast isolates. The phylogenetic analysis classified the isolates into three major clusters. Among the three clusters, cluster one recorded 14 isolates, cluster two consisted of 16 isolates, and cluster three had 2 isolates. Analysis of molecular variance (AMOVA) showed high genetic variation among individuals and less among populations. Principal coordinate analysis (PCoA) showed a 27.16% genetic variation among populations. The present study provides the first report on the genetic diversity and population structure of the foxtail millet infecting *M. grisea* population in Tamil Nadu, which could be useful in developing blast-resistant foxtail millet cultivars.

1 **Analysis of genetic diversity and population structure of *Magnaporthe grisea*, the causal**

2 **agent of foxtail millet blast using microsatellites**

3 Manimozhi Dhivya[a], Govindasamy Senthilraja[b,*], Nagendran Tharmalingam[c, *],

4 Sankarasubramanian Harish[b], Kalaiselvan Saravanakumari[b], Theerthagiri Anand[b],

5 Sundararajan Thiruvudainambi[a]

6

7 [a]Department of Plant Pathology, Agricultural College and Research Institute, Tamil Nadu

8 Agricultural University, Madurai 625104, Tamil Nadu, India,

9 [b]Department of Plant Pathology, Tamil Nadu Agricultural University, Coimbatore 641003, Tamil

10 Nadu, India,

11 [c]Infectious Disease Division, Department of Medicine, The Miriam Hospital/The Rhode Island

12 Hospital, Alpert Medical School of Brown University, Providence. RI- 02903. The USA.

13

14 *Corresponding author: senthilraja@tnau.ac.in, nagendran_tharmaligam@brown.edu

15

16   **Abstract**

17   Foxtail millet blast caused by *Magnaporthe grisea* is becoming a severe problem of foxtail

18   millet farming in all over-regions of India. Information on the genetic diversity and population

19   structure of foxtail millet infecting *M. grisea* is essential for developing effective management

20   strategies, including the breeding of blast-resistant cultivars. We analysed thirty-two *M. grisea*

21   isolates from ten foxtail millet growing districts in Tamil Nadu, India for genetic diversity using

22   twenty-nine microsatellite or Simple Sequence Repeat (SSR) markers in this study. A total of 103

23   alleles were identified, with a mean of 3.55 alleles/locus. Gene diversity ranged from 0.170 to

24   0.717, while major allelic frequencies ranged from 0.344 to 0.906. The polymorphism information

25   content (PIC) value was identified as 0.155 to 0.680, with an average value of 0.465. Population

26   structure analysis of genomic data sets revealed two major populations (SP1 and SP2) with

27   different levels of ancestral admixture among the 32 blast isolates. The phylogenetic analysis

28   classified the isolates into three major clusters. Among the three clusters, cluster one recorded 14

29   isolates, cluster two consisted of 16 isolates, and cluster three had 2 isolates. Analysis of molecular

30   variance (AMOVA) showed high genetic variation among individuals and less among populations.

31   Principal coordinate analysis (PCoA) showed a 27.16% genetic variation among populations. The

32   present study provides the first report on the genetic diversity and population structure of the

33   foxtail millet infecting *M. grisea* population in Tamil Nadu, which could be useful in developing

34   blast-resistant foxtail millet cultivars.

35   **Keywords**: Foxtail millet, diversity, blast, population structure, microsatellites, phylogenetics

36

37

1. INTRODUCTION

Foxtail millet (*Setaria italica* (L.) P. Beauv.) is one of the most important climate-resistant nutri-cereals plants that comprise a vast array of nutritional properties such as protein, starch, fiber, minerals, and antioxidants. It is widely cultivated around the world (Sharma & Niranjan, 2018). The cultivation and consumption of small millet are increasing in Inida. The agro-industry is now focusing to increase the productivity of small millet by implementing appropriate management strategies against yield-limiting factors (Sharma & Niranjan, 2018).

The ascomycetous fungus *Magnaporthe grisea* (T.T. Herbert) M.E. Barr) (anamorph: *Pyricularia grisea* (Cooke.) Sacc.) causes blast disease in various cereals and millets worldwide (Noman et al., 2022; Aravind et al., 2022). The disease has become a significant obstacle in cultivating foxtail millet, particularly in Karnataka, Tamil Nadu, Andhra Pradesh, Rajasthan, Madhya Pradesh, and Chhattisgarh in India (Sharma et al., 2014). The pathogen has a hemibiotrophic and heterothallic lifestyle (Koeck et al., 2011), which affects different parts of the plant, including leaves, leaf sheaths, nodes, necks, heads, or panicles at all stages of plant growth (Wilson & Talbot, 2009). Initially, the disease manifests itself as a small water-soaked lesion, after which the spots turn dark green with a central light green to greyish area. Fully developed spots have a brown to dark brown margin with a white to grey center. During the life cycle, the pathogen produces thin-walled, three-celled, pear-shaped conidia with a protruding hilum at the tips of the conidiophores, which cause and spread disease from one plant to another (Klaubauf et al., 2014).

It is known that blast pathogens develop resistance to fungicides (Suzuki et al., 2010). Therefore, the best way to control this disease is to breed resistant cultivars. However, the pathogen can rapidly evolve to overcome the host plant resistance as different strains and pathotypes are present in the *Magnaporthe* populations in the field (Sharma et al., 2014; Kim et al., 2019). Therefore, it is necessary to analyze the genetic diversity among the *Magnaporthe* populations in a particular region to understand the mechanism of breakdown of resistance in blast-resistant cultivars (Rieux et al. 2011).

Previous studies have demonstrated genetic diversity among blast pathogens in a variety of food crops, including rice (Aravind et al., 2022), wheat (Noman et al., 2022), finger millet (Takan et al., 2012), and pearl millet (Sharma et al., 2021). However, no studies have been conducted on the genetic structure of foxtail millet infecting *Magnaporthe* populations in India. Although the pathogen is variable, it is very host-specific in relation to foxtail millet (Sharma et al., 2014).

69 Improving our understanding of the diversity within and among populations of blast pathogens at
70 the field level is critical to formulating effective management strategies, including the development
71 of blast resistant cultivars of foxtail millet. Among the various tools and methods used to study the
72 genetic diversity of pathogens, microsatellites or simple sequence repeats (SSRs) are the most
73 widely used marker system to study the genetic diversity or evolutionary aspects of organisms
74 (Rieux et al., 2011; Li et al., 2021). The microsatellites or SSRs are tandemly repeated DNA
75 sequences present throughout the eukaryotic genome. In addition, SSR markers have several
76 properties superior to other marker systems, which include being relatively inexpensive (Schoebel
77 et al., 2013), highly polymorphic, multi-allelic, highly reproducible, and user-friendly (Nowicki et
78 al., 2022). Several SSR markers (Kaye et al., 2003) and minisatellite markers (Li et al., 2007) are
79 developed already for *M. grisea*. We aimed to analyze the extent of genetic variability and
80 population structure in field populations of foxtail millet infecting *M. grisea* in Tamil Nadu using
81 SSR markers that we discussed in this study. This is the first report of its kind up to our knowledge
82 on the genetic structure of foxtail millet infecting *M. grisea.*

83 **2. MATERIALS AND METHODS**

84 **2.1. Survey, collection and isolation of *M. grisea***

85 A detailed roving survey was conducted in major foxtail millet growing areas (hills and

86 plains) in Tamil Nadu, India during the rainy season between 2017 and 2018 to assess the severity

87 of blast disease. Blast severity was measured on a 1-9 scale (Sharma et al., 2014) and expressed

88 as a Percent Disease Index (PDI) using the formula PDI = (sum of individual ratings/no. of leaves

89 assessed x maximum disease grade value) x 100 (Wheeler, 1969; Amoghavarsha et al., 2022).

90 Plant samples (leaves and leaf sheaths) infected with blast were collected from the farmers' fields.

91 Collected samples were air dried, bagged, labelled and stored under refrigerated conditions at 4ºC

92 for the isolation of pathogens. The pathogen was isolated using the standard tissue isolation

93 procedure (Tuite, 1969) with Potato Dextrose Agar (PDA) medium under aseptic conditions at

94 $25\pm2°C$. Mycelium growing from infected plant tissue was identified based on its morphological

95 and cultural characteristics. The fungus was then purified by a single spore isolation technique

96 (Ricker & Ricker, 1936) and the purified isolates were stored on PDA slants for further study.

97 **2.2. DNA extraction**

98 Each isolate was inoculated into a 100 ml Erlenmeyer flask containing 20 ml of potato

99 dextrose broth and incubated at $25 \pm 2°C$. After 7 days of incubation, the mycelia were harvested

100 and immediately ground in liquid nitrogen to a fine powder for DNA extraction with CTAB buffer,

101 following the protocol described by Murray & Thompson (1980) with minor modifications

102 (Jagadeesh et al., 2018) using equal volumes of supernatant and a mixture of phenol-chloroform-

103 isoamyl alcohol to precipitate and isolate the DNA from other impurities. The DNA was verified

104 quantitatively and qualitatively using a Nano Drop Spectrophotometer (Themoscientific) and then

105 diluted to a working concentration of 50 ng/µl and stored at -20˚C for later use.

106 **2.3. PCR assays**

107 2.3.1. ITS rDNA amplification

108 All the isolates were subjected to PCR amplification using a pair of universal primers, ITS1

109 and ITS4 (White et al., 1990). Primer sequences were synthesized by Eurofins Genomics India

110 (Bangalore, India). The PCR was performed in 20 µl reaction volume with 2.0 µl template DNA

111 (50 ng/µl), 10.0 µl master mix, 2.0 µl forward primer, 2.0 µl reverse primer and 4.0 µl sterile

112 double-distilled water. The reaction mixture was centrifuged briefly to thoroughly mix the

113 components of the cocktail. Amplification was performed in a thermal cycler (C1000 Touch™

114 Thermal Cycler, Bio-Rad Laboratories, Inc., Singapore). Thermal cycling conditions were
115 achieved consisting of 35 cycles, initial denaturation at 94°C for 5 min, denaturation at 94°C for
116 1min, annealing at 55°C for 1 min, extension at 72°C for 2 min and final extension at 72°C for 5
117 min. The PCR products were subjected to agarose (1%) gel electrophoresis in 0.5X Tris-Borate-
118 EDTA buffer at 110V. A 100 bp DNA molecular ladder (MEDOX Biotech, Chennai, India) was
119 used to estimate the size of the amplicon. After electrophoretic separation, the gel was read under
120 the gel documentation system (Bio Rad, USA) for a more detailed analysis.

121 **2.3.2. Microsatellite genotyping**

122 A total of twenty-nine microsatellite loci (SSRs) distributed across seven *M. grisea*
123 chromosomes were used in this study (Table S1) to analyze genetic diversity and population
124 structure as described by Kaye et al. (2003) and Adreit et al. (2007). These primer sequences were
125 synthesized at Eurofins Genomics India (Bangalore, India). PCR amplification was performed in
126 20 μl of reaction mix in a 0.5 microcentrifuge tube using 10 ng of template DNA, 0.2 mM of
127 dNTPs, 0.4 μM of primers, 1.5 mM MgCl2, 1X Taq buffer (10 mM Tris-HCl, 50 mM KCl, pH
128 8.3) and 1U Taq DNA polymerase (DreamTaq, Thermo Scientific, USA). Conditions for PCR
129 were initial denaturation at 94°C for 5 min, followed by 35 cycles of denaturation at 94°C for
130 30 s, primer annealing at 55°C for 45 s, and extension at 72°C for 45 s, with the final extension for
131 10 min at 72°C. For marker scoring, the PCR products were separated by electrophoresis on a
132 2.5% agarose gel stained with ethidium bromide. After electrophoretic separation, the gels were
133 analysed under the gel documentation system (Biorad, USA). All PCR reactions for each primer
134 were repeated at least twice to confirm the data scored.

135 **2.4. Bioinformatics and computational and statistical analyses**

136 The percent disease index of foxtail millet blast and observations on the conidial morphology
137 of *M. grisea* were subjected to analyses of variance (ANOVA). The averages were compared by
138 the Tukey test ($p < 0.05$) in the Statistical Package for the Social Sciences (SPSS), version 21.0.

139 The amplified PCR products were sequenced at M/S Eurofins Genomics Bangalore, India
140 for double pass DNA sequencing using the universal primers (ITS1 and ITS4) mentioned above.
141 The DNA sequences obtained in this study were subjected to phylogenetic analysis. A neighbor-
142 joining tree (Saitou & Nei, 1987) was constructed with MEGA v 6.1 software to study divergence
143 patterns, and a 1000-repetition bootstrap analysis was performed to support nodes in clusters
144 (Tamura et al., 2011).

145   Basic computational and statistical analyses such as polymorphic information content (PIC),
146   gene diversity, major allele frequency and heterozygosity were analyzed using Power Marker
147   version 3.25 (Liu & Muse, 2005). Pairwise F-statistics, Nei genetic distance, analysis of molecular
148   variance (AMOVA) and principal coordinate analysis (PCoA) were performed using the package,
149   namely GenA1Ex v. 6.502 (Peakall & Smouse, 2006). PIC values measure the significance of a
150   given DNA marker. The PIC value for each SSR locus was measured as described by Anderson et
151   al. (1993). An unweighted neighbor-joining tree was constructed based on the simple matching
152   dissimilarity matrix of SSR markers genotyped across the *M. grisea* isolates as implemented in the
153   DARwin v. 5.0.157 programme (Perrier & Jacquemoud-Collet, 2006). Population structure
154   between *M. grisea* isolates was analyzed with the software package STRUCTURE (Pritchard et
155   al., 2000) in the revised version 2.3.4. This approach makes use of multilocus genotypes to infer
156   the fraction of an isolate's genetic ancestry that belongs to a population for a given number of
157   populations (K). The optimum number of populations (K) was selected after five independent runs
158   of a burn-in of 50,000 iterations followed by 50,000 iterations for each value of K (testing from K
159   = 2 to K = 10). The program STRUCTURE HARVESTER was used to determine the peak value
160   of delta K according to the method described by Evanno et al. (2005).
161

162 **3.   RESULTS**

163 **3.1. Survey and assessment of blast severity in foxtail millet**

164   The prevalence of foxtail millet leaf blast was noticed in all surveyed areas (plains and hills)

165   in Tamil Nadu. Interestingly, the occurrence of sheath blast was noticed only in the Kunnur village,

166   Salem District. The severity of leaf blast disease were ranged from 10.34 to 72.19 PDI. The highest

167   incidence was observed in cv. CO(Te)7 (72.19 PDI) in Athiyandal village, Tiruvannamalai

168   District, followed by a local variety from a farmer's field in Kunnur village, Salem District, which

169   had a PDI of 70.16. The minimum PDI (10.34) was observed in cv. CO(Te)5 in Madurai. Sampling

170   locations were marked on the map of Tamil Nadu using ARC GIS software, and the PDI or blast

171   severity was given in three different colours according to its range. The green colour represents a

172   lesser incidence of the disease in the Salem, Madurai, and Virudhunagar districts. The yellow

173   colour indicates a moderate disease indidence in the Thoothukudi, Dindigul, Erode, Salem,

174   Namakkal, and Dharmapuri districts. The highest incidence of the disease was recorded in Vellore,

175   Tiruvannamalai, Dindigul, and Virudhunagar districts and is marked in red (Figure 1; Table 1). At

176   the time of the survey, the leaf blast was observed by the type of lesion, which was characterized

177   by a spindle-shaped lesion with a dark brown border with a grey center, and the sheath blast

178   symptom was observed as a spindle-shaped lesion with a dark brown border with a white center

179   on the sheath (Figure 2a,b).

180 **3.2. Morphological characterization**

181   A total of 32 isolates of *M. grisea* were isolated from the diseased samples (31 from leaf and

182   1 from sheath) and designated as TNFxM1 to TNFxM32 (Table 1). All isolates were classified

183   based on morphological and conidial characteristics variations, namely colony colour, surface

184   appearance, size, shape, and colour of the conidia. Colony colour varied as greyish brown (15),

185   slightly greyish brown (3), creamish white (1), white (4), greyish white (4), blackish white (3), and

186   greyish black (2). Similarly, most of the isolates were smooth (19) and some were rough (13) in

187   colony appearance (Figure S1; Table 2). In all the isolates, the shape of the conidia was typically

188   pyriform with a rounded base, narrow apex, 2 septa, 3 celled, and the middle cells were broader

189   than the adjacent cells in all the isolates,. Some of them were very long and narrow, while others

190   were quite wide. The length and width of the conidia of different isolates of *M. grisea* were

191   measured (Figure S2; Table 2). The size of the conidia ranged from 20.06 μm to 37.76 μm in length

192   and 6.88 μm to 11.93 μm in width**.** All isolates varied significantly in terms of conidial size. The

193   blast isolates TNFxM7 and TNFxM20 had the longest conidia of 37.76 μm and 33.83 μm,

194   respectively. The shortest conidial length was observed in isolates TNFxM23 (20.06 μm) and

195   TNFxM6 (21.48 μm). The highest conidial width was observed in isolates TNFxM26 and

196   TNFxM27 at 11.93 μm and 10.77 μm, respectively.

197   **3.3. ITS-DNA barcoding and phylogenetic analysis**

198   ITS-based primers amplified the expected amplicon size of 560 bp (Figure S3). All the

199   sequences obtained from this study by partial gene sequencing showed more than 99% sequence

200   similarity to GenBank sequences (*M. grisea*) deposited with the NCBI. Accession numbers

201   obtained from the NCBI GenBank for each isolate are listed in Table 1.

202   The phylogenetic analysis revealed that all 32 *M. grisea* isolates were divided into two

203   groups (Group I and Group II). The two isolates (MN017168 and MN028778) from Virudhunagar

204   District were only clustered separately and formed group I. Group II consists of thirty isolates with

205   a further subdivision into subgroup I and subgroup II. Subgroup I was formed with eight isolates

206   from Tiruvanamalai (MN017167), Salem (MW534814, MW535244, MW504790, MW535295,

207   MW535961 and MW496127) and Namakkal (MW497613) districts. The remaining twenty-two

208   isolates from Dindigul (MT053476, MK990557, MN028779, and MN017169), Thoothukudi

209   (MN028776), Madurai (MT043762 and MT053462), Dharmapuri (MT043764), Vellore

210   (MT043805), Erode (MW497608 and MW534750), Salem (MW534813, MW534870,

211   MW535067, MW535174, MW494605, MW498280, MW504997, MW504990, and MW494316)

212   and Namakkal (MW494589 and MW535771) districts were grouped altogether and formed

213   subgroup II (Figure 3).

214   **3.4. SSR genotyping and cluster analysis**

215   All 32 isolates were genotyped with 29 SSR markers distributed throughout the

216   *M. grisea* genome. A total of 103 alleles were detected among the 29 SSR markers, ranging from

217   2 (Pyrms 67-68, Pyrms 107-108 and Pyrms 533-534) to 6 (Pyrms 607-608) alleles with an average

218   of 3.55 alleles per locus. The major allele frequency ranged from 0.344 (Pyrms 83-84) to 0.906

219   (Pyrms 533-534), with a mean of 0.605. Genetic diversity ranged from 0.170 (Pyrms 533-534) to

220   0.717 (Pyrms 657-658) with a mean value of 0.517. The polymorphism information content (PIC)

221   of the markers had an average value of 0.465 and varied from 0.155 to 0.680. The maximum value

222   of PIC was observed for marker Pyrms 37-38, while the minimum value was observed for marker

223   Pyrms 533-534. The observed mean heterozygosity was 0.007517 with a range of 0.00 to 0.094.

224 Among the markers used, only 5 (Pyrms 37-38, Pyrms 39-40, Pyrms 99-100, Pyrms 427-428, and
225 Pyrms 453-454) showed a heterozygosity value greater than zero, while 24 had zero values (Table
226 3). The unrooted unweighted neighbour Joining method was used to estimate the genetic distance
227 and dissimilarity index of 32 *M. grisea* isolates. For the unrooted tree, isolates were classified into
228 three major clusters (Figure 4). Among the three clusters, cluster one (red colour) recorded 14
229 isolates, while cluster 2 (blue colour) consisted of 16 isolates, and cluster 3 (green colour) had 2
230 isolates.

231 **3.5. Population structure analysis**

232 For genetic structure estimation, a Bayesian clustering approach was followed by taking
233 probable subpopulations (K), and a higher delta K value using STRUCTURE 2.3.6 software. The
234 maximum plateau of *adhoc* measurement of ΔK was K=2 with a ΔK value of 219.8 (Table S2).
235 The population structure was analyzed for genetic relatedness among 32 *M. grisea* isolates
236 collected from ten different districts of Tamil Nadu, India. Based on an ancestry threshold of
237 >70%, all 32 isolates were classified into two major populations and considered pure, while <70%
238 were considered admixture (AD). Among the 32 isolates, 13 isolates collected from Salem and
239 Namakkal districts were classified as subpopulation 1 (SP1), and 16 isolates collected from
240 Tiruvanamalai, Dindigul, Virudhunagar, Thoothukudi, Madurai, Dharmapuri, Vellore, Madurai,
241 Erode and Salem districts were classified as subpopulation 2 (SP2), while 3 isolates (TNFxM6,
242 TNFxM17, and TNFxM18) were of admixture type with a major genetic component of two
243 subgroups (Table 4). The population shows admixture, suggesting that there is a gene flow
244 between these populations. The fixation index (F_{st}) values of the two populations were 0.4296 for
245 SP1 and 0.2021 for SP2. The highest divergence in allele frequency between populations was
246 observed in SP1 and SP2 (0.1077) based on the net nucleotide distance calculated using point
247 estimates of P. The mean distance (expected heterozygosity) between individuals in the panel
248 population was 0.2036 and 0.2800 in response to SP1 and SP2, respectively (Figure 5a,b; Figure
249 S4a-c).

250 **3.6. Analysis of molecular variance (AMOVA)**

251 The two populations, i.e., subpopulation 1 (13), and subpopulation 2 (16), along with the
252 admixtures (3) generated from structure analysis, were analyzed to determine genetic variation
253 among and within populations. In the AMOVA analysis, maximum variation (79%) was found
254 among individuals, while minimum variation (20%) was noticed between the populations and

PeerJ

255   within individuals (1%) (Figure 6; Table S3). The deviation from Hardy-Weinberg's prediction

256   was performed using Wright's F-statistics. The F_{is} and F_{it} values for all 29 loci were found to be

257   0.984 and 0.987 (r = <0.001), respectively, while F_{st} between populations was 0.202. The NM

258   value of assumed subpopulations was noted as 0.989. The highest pairwise genetic Nei distance

259   was observed between SP1 and AD (0.404), followed by SP1 and SP2 (0.362) and SP2 and AD

260   (0.307). Furthermore, the biplot generated from the principal coordinate analysis (PCoA) showed

261   that the first two components account for 100% of the variations (Figure 7a,b). The scatterplot was

262   developed from the PCoA analysis and displayed across isolates on the first two axes. The PCoA

263   1 biplot captured 18.03% of the variation, while PCoA 2 contributed 9.13% to the total genetic

264   variation, suggesting that the total genetic variation among the populations was 27.16% (Table

265   S4a, S4b).

266

4. DISCUSSION

Foxtail millet is grown in both the plain and hilly regions of Tamil Nadu in India. The blast disease caused by *M. grisea* (Sharma et al., 2014), causing a vast yield loss. We examined the morphological and genetic variability of 32 *M. grisea* isolates using 29 microsatellite markers (Kaye et al., 2003; Adreit et al., 2007) and universal ITS primers (ITS1 and ITS4) to characterize the genetic diversity and population structure of foxtail millet infecting *M. grisea*. We demonstrated the genetic analyses of foxtail millet blast populations, which can be used to develop blast-resistant foxtail millet cultivars.

In the present study, the severity of the blast was assessed in various foxtail millet growing areas in Tamil Nadu during the rainy season between 2017 and 2018. The highest incidence of the disease was observed in the Vellore, Tiruvannamalai, Dharmapuri, and Dindigul districts of Tamil Nadu. Similarly, Sharma et al. (2014) also noticed the occurrence of blast incidence during the rainy season in 2008 in different foxtail millet growing tracts in Telangana and Andhra Pradesh. We isolated the causative agent of foxtail millet blast from the infected leaf and sheath samples collected at surveyed fields using PDA medium and purified by the single spore isolation technique. Other reports demonstrating that a similar single-spore isolation technique was used to isolate and purify *Magnaporthe* from rice, wheat, finger millet and foxtail millet using different media (Sharma et al., 2014; Yadav et al., 2019) were discussed and corroborate to our study.

The present study demonstrates a variation in mycelium colour and texture variation among the 32 fungal isolates collected in Tamil Nadu. This confirms previous reports by Panda et al. (2017) and Sahu et al. (2018), who classified the rice blast isolates collected from different parts of Chhattisgarh and Odisha in India into different groups based on colony colour and texture. The present study shows the variation among the 32 isolates of *M. grisea* in terms of morphological and conidial characteristics. However, there is no significant difference between the colony morphology and conidial characters concerning the collection period and geographical distribution of the isolates.

Sequencing of the ITS region of rDNA has become the universal barcode system for identifying fungal taxonomy at the species level (Paloi et al., 2022). In the present study, all *M. grisea* isolates were amplified using universal primers (ITS1 and ITS4) and the result showed the expected 560 bp amplicon in all isolates. The isolates showed a sequence homology of >99% with *M. grisea*. The results of the present study are consistent with Jagadeesh et al. (2018) who

298   examined the diversity of 72 isolates of *M. oryzae* collected in Karnataka, India using primers
299   ITS1 and ITS4.

300   Microsatellites or SSRs are powerful markers used for the population genetic analyses due
301   to their high specificity, polymorphism and reproducibility (Schoebel et al., 2013; Nowicki et al.,
302   2022). We evaluated 29 SSR markers reported by Kaye et al. (2003) and Adreit et al. (2007) to
303   analyze genetic diversity in the population of foxtail millet infecting *M. grisea* from Tamil Nadu.
304   To the best of our knowledge, this is the first study to investigate the molecular diversity and
305   population structure of 32 isolates of foxtail millet infecting *M. grisea* from Tamil Nadu using
306   microsatellites. The SSR markers used in this study varied widely and the results were generally
307   consistent with previous population genetic studies conducted in India and elsewhere (Yadav et
308   al., 2019). In the present study, 103 alleles were detected using 29 microsatellite markers. The
309   number of alleles per locus ranged from 2 to 6, averaging 3.55 alleles/locus. A variation in the
310   number of alleles was observed between the markers used. Previous studies reported similar results
311   in rice (Aravind et al., 2022), wheat (Noman et al., 2022), finger millet (Takan et al., 2012), and
312   pearl millet (Sharma et al., 2021) infecting populations of *Magnaporthe* in different geographic
313   locations. Some previous studies showed that the high number of alleles per locus resulted in high
314   genetic variation. The high genetic diversity was demonstrated in the present study, confirming
315   previous results of Saleh et al. (2014), while Yadav et al. (2019) reported a low level of genetic
316   diversity among the *M. oryzae* isolates collected in North Eastern India.
317   Similarly, high levels of polymorphism were found among the 29 microsatellites used in this
318   study. The results agree with Wang et al. (2017), where a high degree of polymorphism was
319   observed when analyzing 457 rice blast isolates collected in the United States using ten SSR
320   markers. Recently, Adhikari et al. (2020) also observed high levels of polymorphism when
321   analyzing 17 pearl millet blast isolates collected in India using SSR markers. However, the low
322   level of polymorphism has been observed in the rice blast population in Brazil and Japan (Prabhu
323   et al., 2002). Analysis of genetic diversity showed the high percentage of identical alleles,
324   indicating considerable gene flow between all isolates of *M. grisea* population in Tamil Nadu.
325   As most foxtail millet cultivation in Tamil Nadu is dominated by a single cultivar CO(Te)7
326   and no resistant cultivar is grown yet, so there is no selection pressure on the pathogen to induce
327   change. Hence this could be why there is a high percentage of identical alleles between populations
328   of *M. grisea*. The present study undoubtedly shows an excellent diversity of *M. grisea* in the hilly

329 region and that most of the variability was within individuals. Our results agree with those of

330 Wang et al. (2017), who analyzed 457 rice blast isolates using the neighbour joining method to

331 build an unrooted tree. A total of five major clusters were identified. The observed clusters were

332 mainly related to the sampling period but not to the geographic location of the isolates.

333   A Bayesin clustering approach was used to analyze the structure of the foxtail millet blast

334 isolates. The structure analysis divided the *M. grisea* isolates into two subpopulations (K=2) with

335 three admixtures. The first subpopulation (SP1) consisted of isolates from the Salem and

336 Nammakal districts of Tamil Nadu. Similarly, the second subpopulation (SP2) consisted of

337 Tiruvannamalai, Madurai, Dindigul, Erode, Virudhunagar, Tuticorin, Dharmapuri, Vellore, and

338 Salem districts in Tamil Nadu. Admixtures (AD) present in isolates can increase genetic diversity.

339 However, the structure analysis could not differentiate the blast isolates based on the geographic

340 location. Similarly, Yadav et al. (2019) identified two subpopulations of leaf and neck blast isolates

341 infecting rice crops and showed limited categorization of blast isolates based on the location.

342 Interestingly, Onaga et al. (2015) categorized the 88 rice blast isolates collected from East Africa

343 into five ancestral genetic clusters (K=5) with Structure V 2.3. Package. Wang et al. (2017)

344 analyzed 457 blast isolates using ten polymorphic microsatellites. They identified 6 genetic

345 clusters (K=6) based on collection period but not geographic location. However, a PCoA analysis

346 was performed from the results obtained from interpreting the structure. The AMOVA analysis

347 was worked out by dividing the genetic diversity within and between the populations of 32 isolates

348 of foxtail millet blast. Variation between these populations contributed 20% of the genetic

349 diversity, while 79% of the genetic variation was present between the individuals; however, one

350 percent of the variation was found within individuals. A higher genetic diversity was found among

351 the blast isolates than in the population. Identically, analysis of molecular variance values for

352 genetic diversity in the pathogen population varied from 78.66% (Wang et al., 2017) to 86.6%

353 (D'Ávila et al., 2016), 88.09% (Onaga et al., 2015) and 98% (Yadav et al., 2019). Our results are

354 consistent with previous reports in which the pathogen population was not differentiated by

355 geographic location (Onaga et al., 2015).

356   The genetic variation and population structure of *M. grisea* infecting foxtail millet from

357 different regions of Tamil Nadu shows significant genetic variation within populations, similar to

358 those observed in other population studies of *M. grisea* in India and elsewhere. Our results showed

359 that gene flow occurs between regions and has significant implications for foxtail millet growers

360 when virulent or fungicide-resistant strains move between regions. Preventing such a threat from

361 the foxtail millet blast requires proper prediction and forecasting systems. In addition, long-term

362 monitoring is essential to identify the population origin and evolutionary potential of foxtail millet

363 blast isolates in India.

364 **ACKNOWLEDGEMENTS**

371 **DATA AVAILABILITY STATEMENT**

372   The data that support the findings of this study are available from the corresponding author

373 upon reasonable request.

374

375 **REFERENCES**

376 Adhikari, S., Joshi, S.M., Athoni, B.K., Patil, P.V. & Jogaiah, S. (2020) Elucidation of genetic
377   relatedness of *Magnaporthe grisea*, an incitant of pearl millet blast disease by molecular
378   markers associated with virulence of host differential cultivars. *Microbial Pathogenesis*,
379   *149*, 104533.

380 Adreit, H., Santoso, Andriantsimialona, D., Utami, D.W., Notteghem, J.L., Lebrun, M.H. &
381   Tharreau, D. (2007) Microsatellite markers for population studies of the rice blast fungus,
382   *Magnaporthe grisea*. *Molecular Ecology Notes*, *7*, 667-670.

383 Amoghavarsha, C., Pramesh, D., Sridhara, S., Patil, B., Shil, S., Naik, G.R., Naik, M.K., Shokralla,
384   S., El-Sabrout, A.M., Mahmoud, E.A. & Elansary, H.O. (2022) Spatial distribution and
385   identification of potential risk regions to rice blast disease in different rice ecosystems of
386   Karnataka. *Scientific Reports*, *12*, 1-14.

387 Anderson, J.A., Churchill, G.A., Autroque, J.E., Tanksley, S.D. & Swells, M.E. (1993) Optimising
388   selection for plant linkage map. *Genome*, *36*, 181-186.

389 Aravind, K., Rajeswari, B., Babu, T.K. & Pushpavalli, S.N.C.V.L. (2022) Pathogenic and
390   molecular variability of *Magnaporthe oryzae* isolates collected from major rice growing
391   locations of Telangana State, India. *Indian Phytopathology*, 1-11.

392 D'Ávila, L.S., Lehner, M.S., Filippi, M.C.C., Scheuermann, K.K. & Del Ponte, E.M. (2016)
393   Genetic structure and mating type analysis of the *Pyricularia oryzae* population causing
394   widespread epidemics in southern Brazil. *Tropical Plant Pathology*, *41*, 297-305.

395 Evanno, G., Regnaut, S. & Goudet, J. (2005) Detecting the number of clusters of individuals using
396   the software STRUCTURE: a simulation study. *Molecular ecology*, *14*, 2611-2620.

397 Jagadeesh, D., Kumar, M.P., Chandrakanth, R. & Devaki, N.S. (2018) Molecular diversity of
398   internal transcribed spacer among the monoconidial isolates of *Magnaporthe oryzae*
399   isolated from rice in Southern Karnataka, India. *Journal of Genetic Engineering and*
400   *Biotechnology*, *16*, 631-638.

401 Kaye, C., Milazzo, J., Rozenfeld, S., Lebrun, M.H. & Tharreau, D. (2003) The development of
402   simple sequence repeat markers for *Magnaporthe grisea* and their integration into an
403   established genetic linkage map. *Fungal Genetics and Biology*, *40*, 207-214.

404   Kim, K.T., Ko, J., Song, H., Choi, G., Kim, H., Jeon, J., Cheong, K., Kang, S. & Lee, Y.H. (2019)
405   Evolution of the genes encoding effector candidates within multiple pathotypes of
406   *Magnaporthe oryzae. Frontiers in microbiology*, *10*, 2575.

407   Klaubauf, S., Tharreau, D., Fournier, E., Groenewald, J. Z., Crous, P. W., De Vries, R. P. &
408   Lebrun, M. H. (2014) Resolving the polyphyletic nature of *Pyricularia* (Pyriculariaceae).
409   *Studies in Mycology*, *79*, 85-120.

410   Koeck, M., Hardham, A. R. & Dodds, P. N. (2011) The role of effectors of biotrophic and
411   hemibiotrophic fungi in infection. *Cellular microbiology*, *13*, 1849-1857.

412   Li, C.Y., Li, J.B., Liu, L., Yang, J., Su, Y., Wang, Y.Y., Xie, Y., Ye, M. & Zhu, Y.Y. (2007)
413   Development of minisatellite markers in phytopathogenic fungus, *Magnaporthe grisea*.
414   *Molecular Ecology Notes*, *7*, 978-980.

415   Li, X., Tao, F., Fan, S., Li, H., Yang, J. & Gao, L. (2021) Genetic diversity of *Venturia inaequalis*
416   isolates (Apple scab) in China and UK determined by SSR markers. *PloS one*, *16*,
417   e0252865.

418   Liu, K. & Muse, S. V. (2005) PowerMarker: an integrated analysis environment for genetic marker
419   analysis. *Bioinformatics*, *21*, 2128-2129.

420   Murray, M. G. & Thompson, W. (1980) Rapid isolation of high molecular weight plant DNA.
421   *Nucleic Acids Research*, *8*, 4321-4326.

422   Noman, M., Al, A., Hosen, S. & Shamsi, S. (2022) Elucidating genetic diversity and population
423   structure of *Pyricularia oryzae* isolates causing wheat blast in Bangladesh. *Archives of*
424   *Microbiology*, *204*, 1-10.

425   Nowicki, M., Hadziabdic, D., Trigiano, R.N., Runge, F., Thines, M., Boggess, S.L., Ristaino, J. &
426   Spring, O. (2022) Microsatellite markers from *Peronospora tabacina*, the cause of blue
427   mold of tobacco, reveal species origin, population structure, and high gene flow.
428   *Phytopathology*, *112*, 422-434.

429   Onaga, G., Wydra, K., Koopmann, B., Séré, Y. & von Tiedemann, A. (2015) Population structure,
430   pathogenicity, and mating type distribution of *Magnaporthe oryzae* isolates from East
431   Africa. *Phytopathology*, *105*, 1137-1145.

432   Paloi, S., Luangsa-ard, J. J., Mhuantong, W., Stadler, M. & Kobmoo, N. (2022) Intragenomic
433   variation in nuclear ribosomal markers and its implication in species delimitation,

434   identification and barcoding in Fungi. *Fungal Biology Reviews*.
435   https://doi.org/10.1016/j.fbr.2022.04.002.

436   Panda, G., Sahu, C., Yadav, M.K., Aravindan, S., Umakanta, N., Raghu, S., Prabhukarthikeyan,
437   S.R., Lenka, S., Tiwari, J.K., Kar, S. & Jena, M. (2017) Morphological and molecular
438   characterization of *Magnaporthe oryzae* from Chhattisgarh. *ORYZA-An International*
439   *Journal on Rice*, *54*, 330-336.

440   Peakall, R.O.D. & Smouse, P. E. (2006) GENALEX 6: genetic analysis in Excel. Population
441   genetic software for teaching and research. *Molecular Ecology Notes*, *6*, 288-295.

442   Perrier, X. & Jacquemoud-Collet, J.P. (2006) DARwin software. http://darwin.cirad.fr/.

443   Prabhu, A.S., Filippi, M.C. & Araujo, L.G. (2002) Pathotype diversity of *Pyricularia grisea* from
444   improved upland rice cultivars in experimental plots. *Fitopatologia Brasileira*, 27, 468-
445   473.

446   Pritchard, J. K., Stephens, M. & Donnelly, P. (2000) Inference of population structure using
447   multilocus genotype data. *Genetics*, *155*, 945-959.

448   Ricker, A.J. & Ricker, R.S. (1936) Introduction to research on plant diseases. Jon. S. *Swift Co.*
449   *Inc., St. Lovis, Chicago, New York, 117*.

450   Rieux, A., Halkett, F., De Lapeyre de Bellaire, L., Zapater, M. F., Rousset, F., Ravigné, V. &
451   Carlier, J. (2011) Inferences on pathogenic fungus population structures from microsatellite
452   data: new insights from spatial genetics approaches. *Molecular Ecology*, *20*, 1661-1674.

453   Sahu, C., Yadav, M.K., Panda, G., Aravindan, S., Umakanta, N., Raghu, S., Prabhukarthikeyan,
454   S.R., Keerthana, U., Adak, T., Sharma, V. & Mohanty, M.R. (2018) Morphological and
455   molecular characterization of *Magnaporthe oryzae* causing rice blast disease in Odisha.
456   *ORYZA-An International Journal on Rice*, *55*, 467-472.

457   Saitou, N. & Nei, M. (1987) The neighbor-joining method: a new method for reconstructing
458   phylogenetic trees. *Molecular Biology and Evolution*, *4*, 406-425.

459   Saleh, D., Milazzo, J., Adreit, H., Fournier, E. & Tharreau, D. (2014) South-East Asia is the center
460   of origin, diversity and dispersion of the rice blast fungus, *Magnaporthe oryzae*. *New*
461   *Phytologist*, *201*, 1440-1456.

462   Schoebel, C.N., Brodbeck, S., Buehler, D., Cornejo, C., Gajurel, J., Hartikainen, H., Keller, D.,
463   Leys, M., Říčanová, Š., Segelbacher, G. & Werth, S. (2013) Lessons learned from

464   microsatellite development for nonmodel organisms using 454 pyrosequencing. *Journal of*
465   *Evolutionary Biology*, *26*, 600-611.

466 Sharma, N. & Niranjan, K. (2018) Foxtail millet: Properties, processing, health benefits, and uses.
467   *Food Reviews International*, *34*, 329-363.

468 Sharma, R., Girish, A.G., Upadhyaya, H.D., Humayun, P., Babu, T.K., Rao, V.P. & Thakur, R.
469   (2014) Identification of blast resistance in a core collection of foxtail millet germplasm.
470   *Plant Disease*, *98*, 519-524.

471 Sharma, R., Goud, T.Y., Prasad, Y.P., Nimmala, N., Kadvani, D.L., Mathur, A.C., Thakare, C.S.,
472   Devi, G.U. & Naik, M.K. (2021) Pathogenic variability amongst Indian isolates of
473   *Magnaporthe grisea* causing blast in pearl millet. *Crop Protection*, *139*, 105372.

474 Suzuki, F., Yamaguchi, J., Koba, A., Nakajima, T. & Arai, M. (2010) Changes in fungicide
475   resistance frequency and population structure of *Pyricularia oryzae* after discontinuance of
476   MBI-D fungicides. *Plant Disease*, *94*, 329-334.

477 Takan, J.P., Chipili, J., Muthumeenakshi, S., Talbot, N.J., Manyasa, E.O., Bandyopadhyay, R.,
478   Sere, Y., Nutsugah, S.K., Talhinhas, P., Hossain, M. & Brown, A.E. (2012) *Magnaporthe*
479   *oryzae* populations adapted to finger millet and rice exhibit distinctive patterns of genetic
480   diversity, sexuality and host interaction. *Molecular Biotechnology*, *50*, 145-158.

481 Tamura, K., Peterson, D., Peterson, N., Stecher, G., Nei, M. & Kumar, S. (2011) MEGA5:
482   molecular evolutionary genetics analysis using maximum likelihood, evolutionary
483   distance, and maximum parsimony methods. *Molecular Biology and Evolution*, *28*, 2731-
484   2739.

485 Tuite, J. (1969) Plant Pathological Methods. Fungi and Bacteria. *Minnesota, USA: Burgess*
486   *Publishing Company*.

487 Wang, X., Jia, Y., Wamishe, Y., Jia, M. H., & Valent, B. (2017) Dynamic changes in the rice blast
488   population in the United States over six decades. *Molecular Plant-Microbe Interactions*,
489   *30*, 803-812.

490 Wheeler, B.E.J. (1969) An introduction to plant diseases. *John Wiley and Sons Ltd., London*.

491 White, T.J., Bruns, T., Lee, S.J.W.T. & Taylor, J. (1990) Amplification and direct sequencing of
492   fungal ribosomal RNA genes for phylogenetics. *PCR protocols: a guide to methods and*
493   *applications*, *18*, 315-322.

494 Wilson, R.A. & Talbot, N.J. (2009) Under pressure: investigating the biology of plant infection by

495   *Magnaporthe oryzae*. *Nature Reviews Microbiology*, *7*, 185-195.

496 Yadav, M.K., Aravindan, S., Raghu, S., Prabhukarthikeyan, S.R., Keerthana, U., Ngangkham, U.,

497   Pramesh, D., Banerjee, A., Adak, T., Kar, M.K. & Parameswaran, C. (2019) Assessment

498   of genetic diversity and population structure of *Magnaporthe oryzae* causing rice blast

499   disease using SSR markers. *Physiological and Molecular Plant Pathology*, *106*, 157-165.

500

501 **FIGURE LEGENDS**

502 FIGURE 1. Map showing the collection sites of *Magnaporthe grisea* isolates and foxtail millet

503   blast severity in Tamil Nadu.

504 FIGURE 2. Foxtail millet blast symptoms. (a) Leaf blast: spindle shaped lesion having dark brown

505   margin with grey coloured center, (b) Sheath blast: spindle shaped lesion having dark

506   brown margin with white coloured center.

507 FIGURE 3. Phylogenetic analysis. Phylogenetic tree constructed based on multiple alignments of

508   nucleotide sequences of *M. grisea* isolates. The tree was generated using the neighbor

509   joining method with 1000 bootstrap replications and the tree drawn at a cut-off value of

510   60% in MEGA 6.1.

511 FIGURE 4. Cluster analysis. Neighbor–joining cluster analysis of 32 blast isolates based on 29

512   SSR markers using DARwin software.

513 FIGURE 5. Population structure analysis. (a) Values of DK, with its modal value used to detect

514   true K of the group (K =2). For each K value, at least three independent runs were

515   considered and averaged over the replicates, (b) Population structure of 32 blast isolates

516   based on 29 markers (K = 2) and graph of estimated membership fraction for K = 2. The

517   maximum of *adhoc* measure ΔK determined by structure harvester was found to be K =

518   2, which indicated that the entire population can be grouped into two subgroups.

519   Different colour within group indicates the proportion of shared ancestry with other

520   group which has the same colour with the admixture.

521 FIGURE 6. AMOVA analysis of foxtail millet infecting *M. grisea* isolates.

522 FIGURE 7. Principal coordinate analysis (PCoA). (a) PCoA for Nei genetic diversity among the

523   three population, (b) PCoA of 32 blast isolates in the panel population using 29

524   molecular markers. The isolates are coloured on the basis of sub-populations obtained

525   from structure analysis (SP1- yellow, SP2 - green, AD - red).

526

527 **SUPPORTING INFORMATION LEGENDS**

528 FIGURE S1. Colony morphology of *M. grisea* isolates. Variability in morphology and cultural
529   characters of *M. grisea* isolates on PDA.

530 FIGURE S2. Conidial characteristics of *M. grisea* isolates. Variation in conidia shapes and sizes
531   among the isolates of *M. grisea* observed under image analyzer.

532 FIGURE S3. PCR amplification of *M. grisea* using ITS Primers (ITS1 and ITS4).

533 FIGURE S4. Population structure analysis. (a) Histogram distribution of Fst1, (b) Histogram
534   distribution of Fst2, (c) Histogram distribution of alpha.
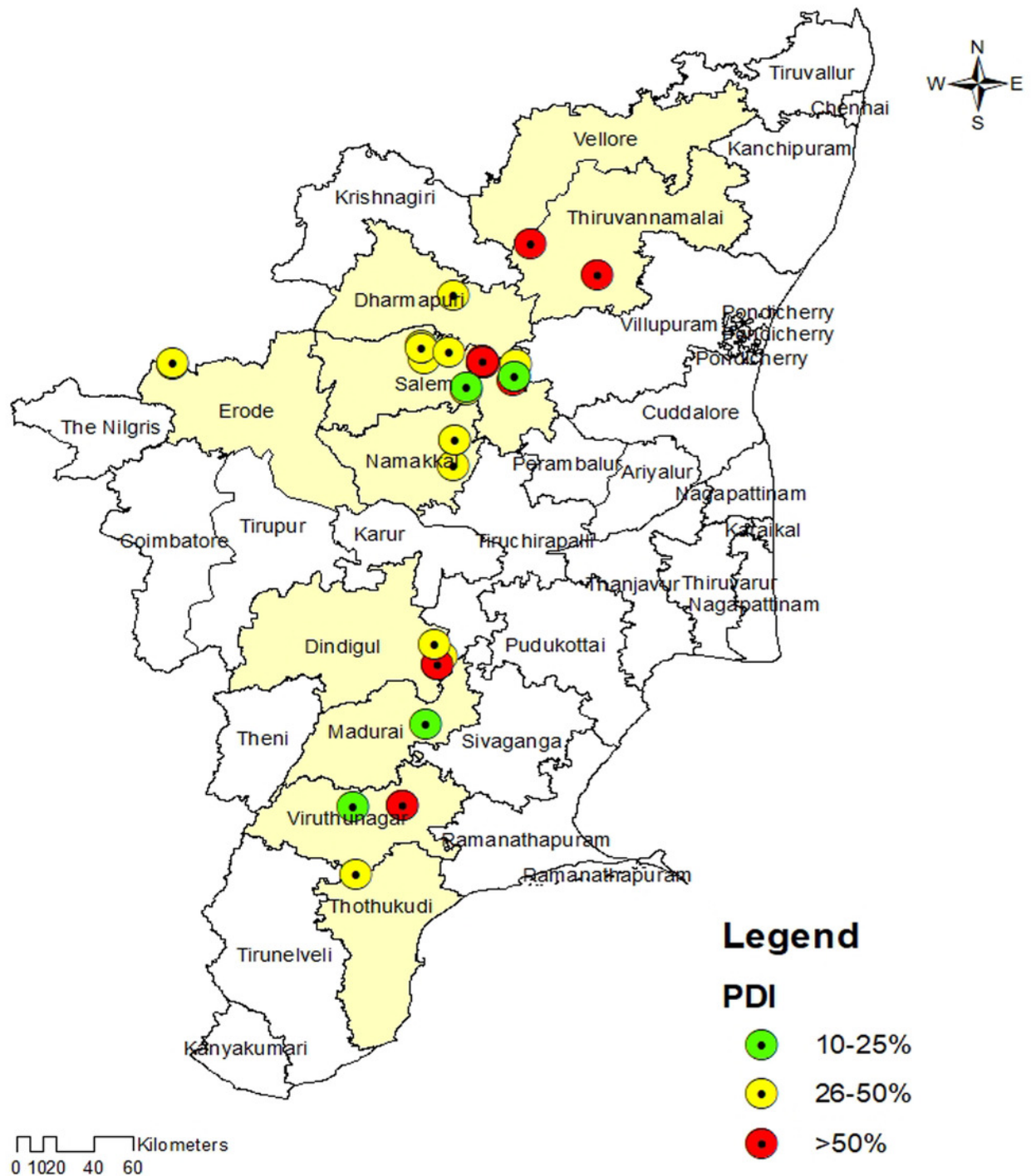
535

536

537

538

Figure 1

Figure 1

Map showing the collection sites of *Magnaporthe grisea* isolates and foxtail millet blast severity in Tamil Nadu

Legend

PDI
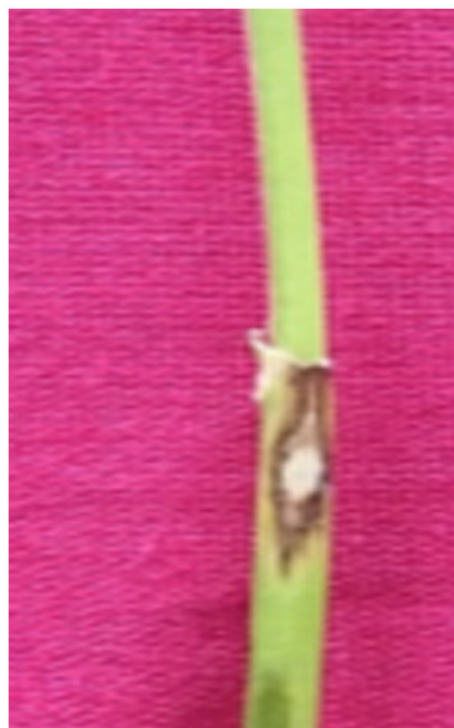
🟢 10-25%

🟡 26-50%

🔴 >50%

Figure 2

Figure 2

Foxtail millet blast symptoms. (a) Leaf blast: spindle shaped lesion having dark brown margin with grey coloured center, (b) Sheath blast: spindle shaped lesion having dark brown margin with white coloured center

(a)

(b)

Figure 3

Figure 3

Phylogenetic analysis. Phylogenetic tree constructed based on multiple alignments of nucleotide sequences of *M. grisea* isolates. The tree was generated using the neighbor joining method with 1000 bootstrap replications and the tree drawn at a cut-off value of 60% in MEGA 6.1.
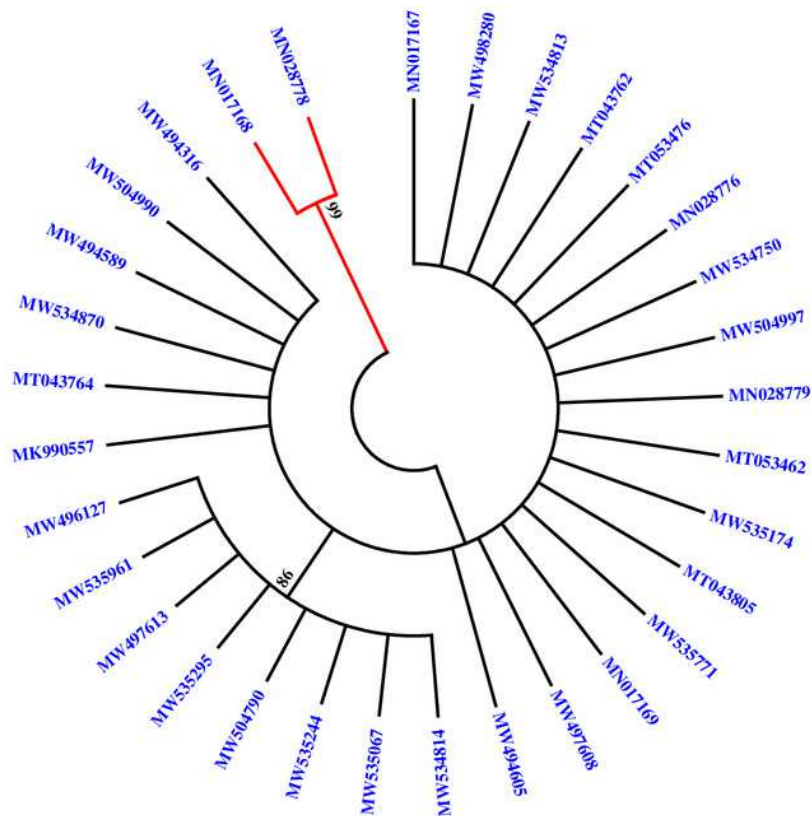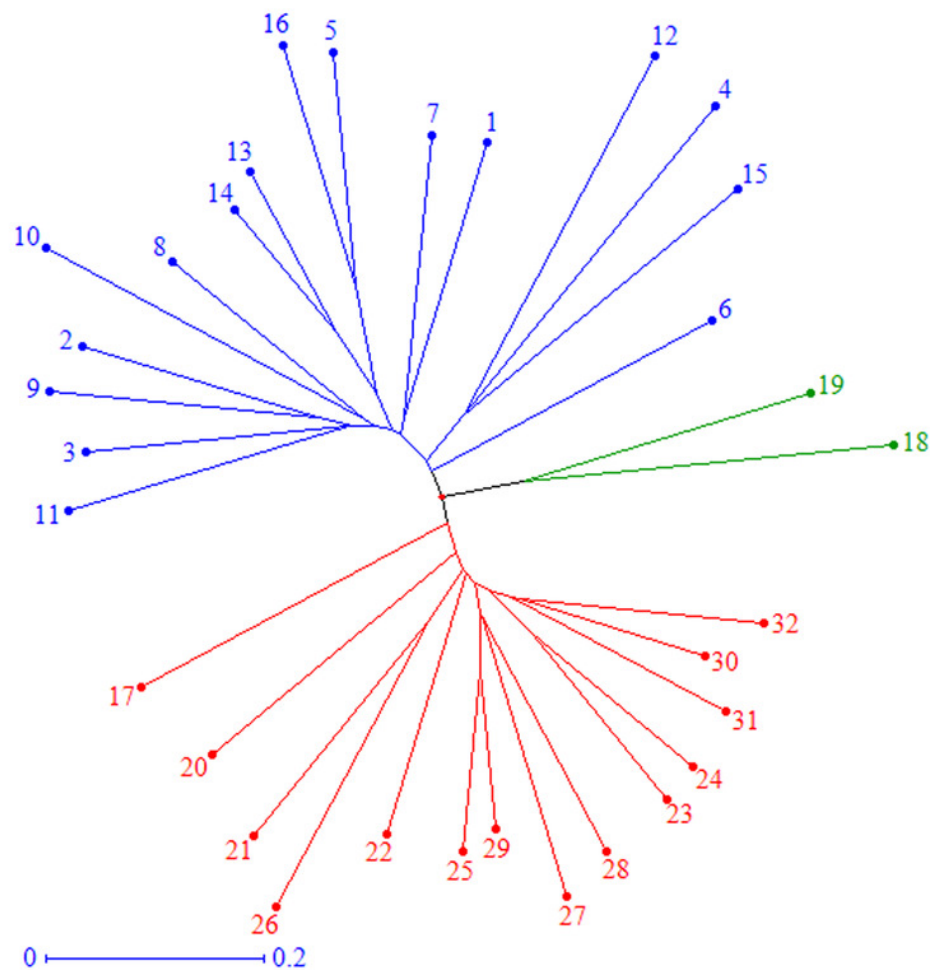
Figure 4

Figure 4

Cluster analysis. Neighbor–joining cluster analysis of 32 blast isolates based on 29 SSR markers using DARwin software

Figure 5

Figure 5

Population structure analysis. (a) Values of DK, with its modal value used to detect true K of the group (K =2). For each K value, at least three independent runs were considered and averaged over the replicates, (b) Population structure of 32 blast isolates based on 29 markers (K = 2) and graph of estimated membership fraction for K = 2. The maximum of *adhoc* measure ΔK determined by structure harvester was found to be K = 2, which indicated that the entire population can be grouped into two subgroups. Different colour within group indicates the proportion of shared ancestry with other group which has the same colour with the admixture.

(a)

DeltaK = mean(|L''(K)|) / sd(L(K))
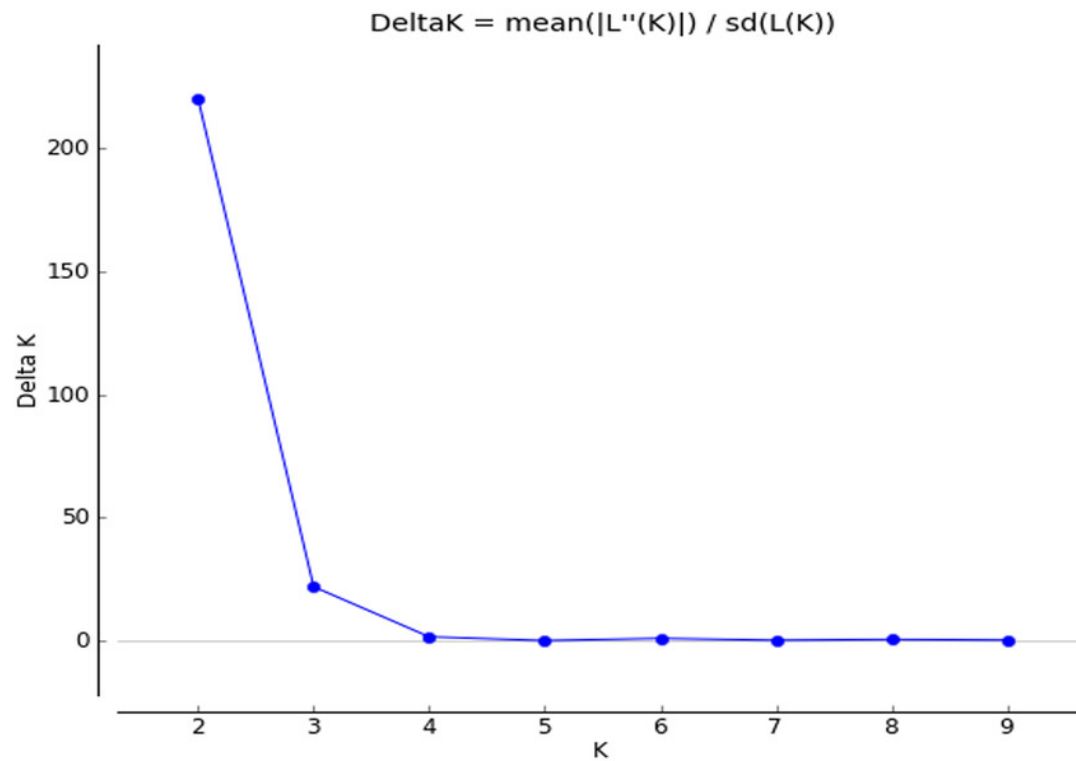
(b)
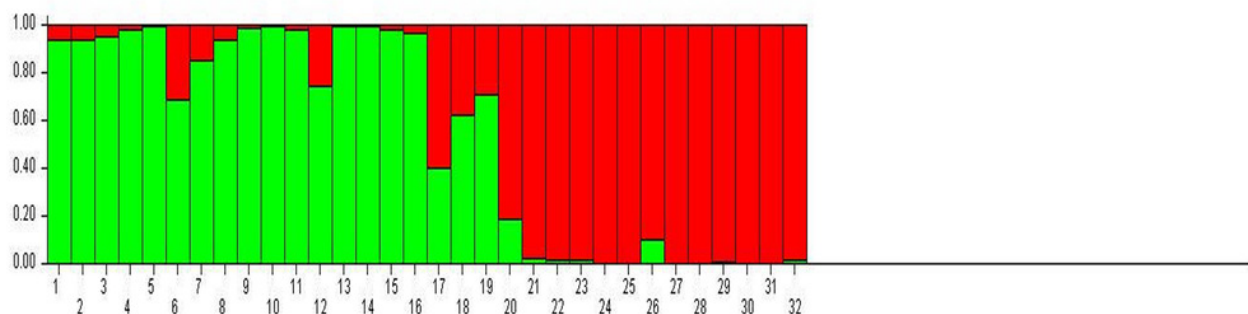
Figure 6

Figure 6

AMOVA analysis of foxtail millet infecting *M. grisea* isolates.
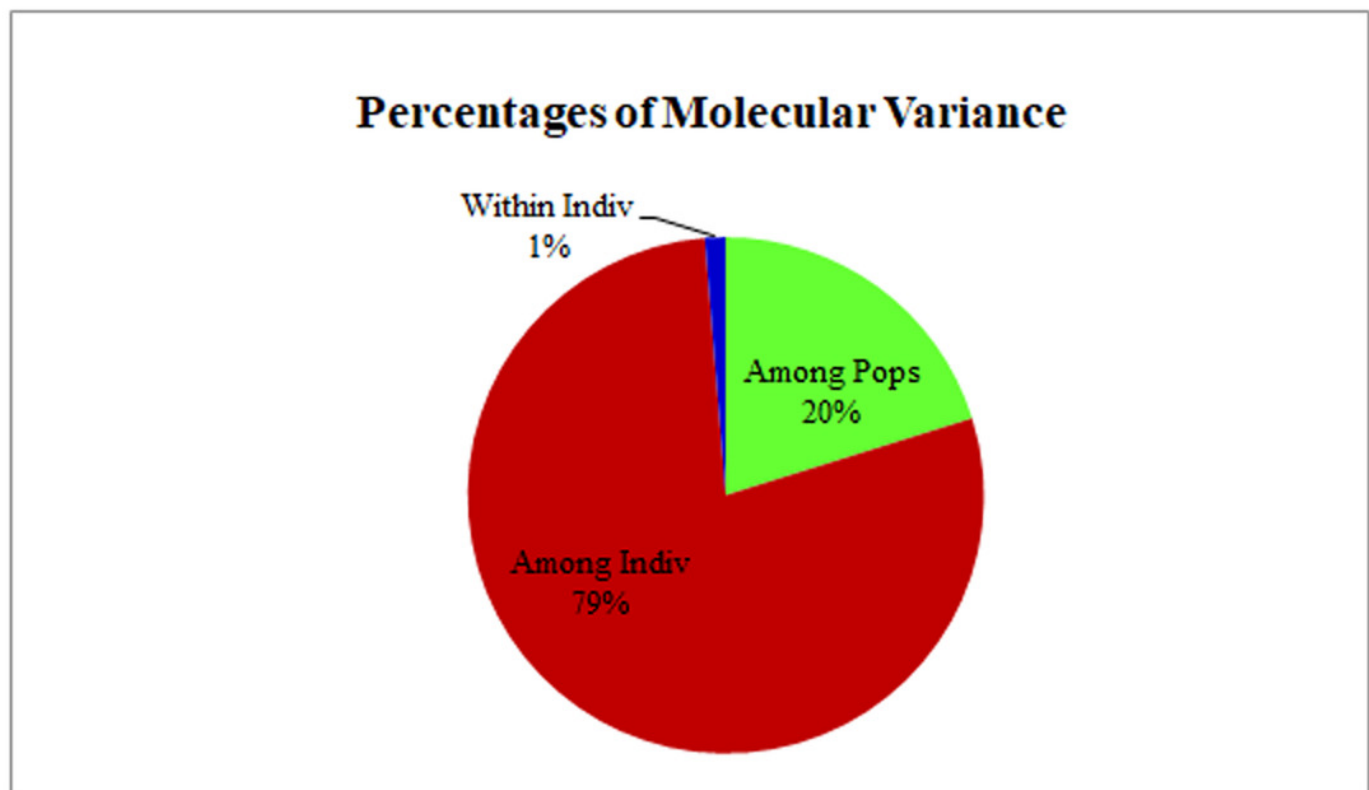
Figure 7

Figure 7

Principal coordinate analysis (PCoA). (a) PCoA for Nei genetic diversity among the three population, (b) PCoA of 32 blast isolates in the panel population using 29 molecular markers. The isolates are coloured on the basis of sub-populations obtained from structure analysis (SP1- yellow, SP2 - green, AD - red).

(a)
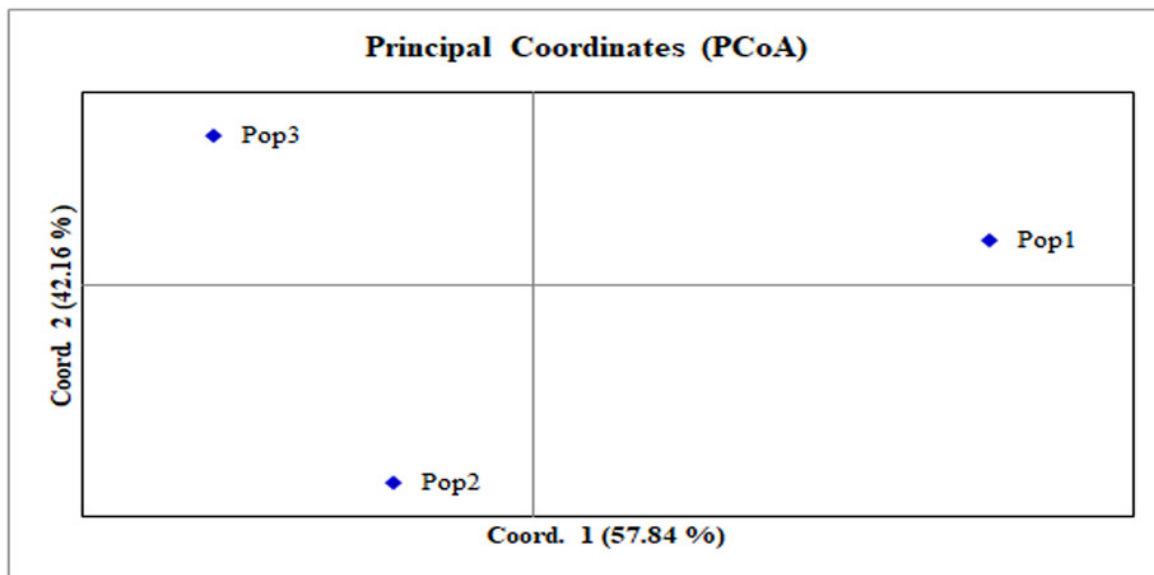
(b)
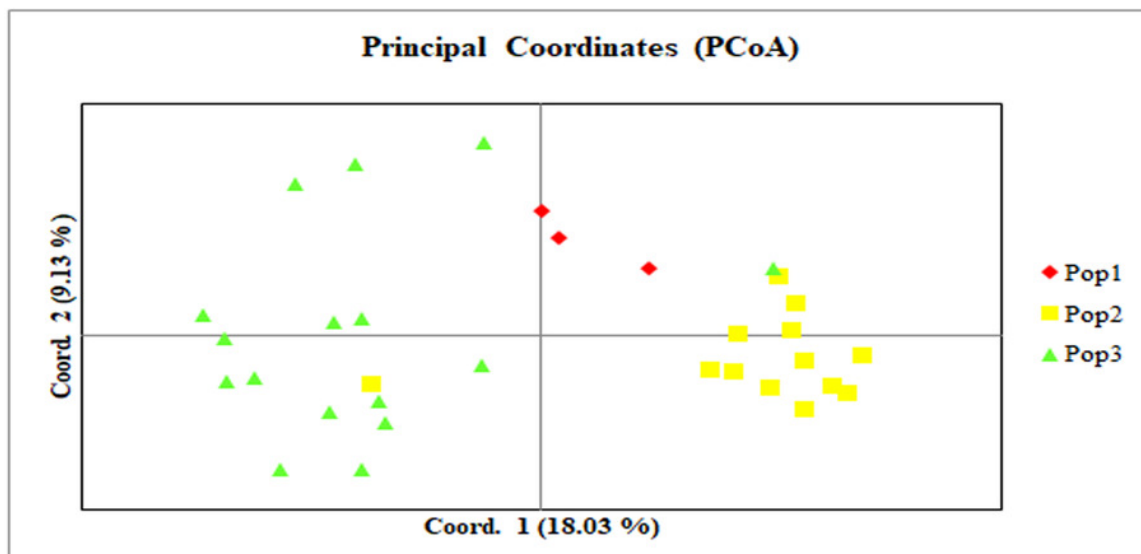
Table 1(on next page)

TABLE 1.

Survey and collection of *M. grisea* isolates from different foxtail millet growing regions of Tamil Nadu

1 TABLE 1. Survey and collection of *M. grisea* isolates from different foxtail millet growing regions of Tamil Nadu

S. No	Year	Isolate code	Topo-graphy	Location	District	Cultivar	PDI	Geographical information		GenBank accession number
								Latitude	Longitude	
1.	2017	TNFxM1	Plains	Athiyandal	Tiruvanamalai	CO(Te)7	72.19^a	12.13°N	79.10°E	MN017167
2.	2017	TNFxM2	Plains	K. Pudhur	Dindigul	Local	64.65^d	10.15°N	78.15°E	MT053476
3.	2017	TNFxM3	Plains	Methugumalai	Dindigul	Local	38.90^i	10.18°N	78.16°E	MK990557
4.	2017	TNFxM4	Plains	K. Pudhur	Dindigul	Local	67.20^c	10.15°N	78.15°E	MN028779
5.	2017	TNFxM5	Plains	Seithur	Dindigul	Local	40.19^i	10.22°N	78.14°E	MN017169
6.	2017	TNFxM6	Plains	Aruppukottai	Virudhunagar	CO(Te)5	68.90^{bc}	09.33°N	78.50°E	MN017168
7.	2017	TNFxM7	Plains	Aruppukottai	Virudhunagar	CO(Te)7	67.98^{bc}	09.33°N	78.50°E	MN028778
8.	2017	TNFxM8	Plains	Kovilpatti	Thoothukudi	CO(Te)7	35.18^j	09.12°N	77.52°E	MN028776
9.	2017	TNFxM9	Plains	Thummakundu	Madurai	Local	21.35^m	09.53°N	77.51°E	MT043762
10.	2017	TNFxM10	Plains	Gobinathampatti	Dharmapuri	Local	35.82^j	12.70°N	78.20°E	MT043764
11.	2017	TNFxM11	Hills	Pudhurnadu	Vellore	Local	59.12^e	12.23°N	78.42°E	MT043805
12.	2017	TNFxM12	Plains	Madurai	Madurai	CO(Te)5	10.34^n	09.58°N	78.12°E	MT053462
13.	2017	TNFxM13	Hills	Thalavadi	Erode	Local	46.67^h	11.46°N	77.00°E	MW497608
14.	2017	TNFxM14	Hills	Thalavadi	Erode	Local	48.12^{gh}	11.47°N	77.00°E	MW534750
15.	2018	TNFxM15	Hills	Kolakoor	Salem	Local	29.45^k	11.48°N	78.12°E	MW534813
16.	2018	TNFxM16	Hills	Suraikayapatti	Salem	Local	30.65^k	11.52°N	78.11°E	MW534814
17.	2018	TNFxM17	Hills	Nagalur	Salem	Local	30.98^k	11.51°N	78.11°E	MW534870
18.	2018	TNFxM18	Hills	Maramangalam	Salem	Local	34.12^j	11.50°N	78.18°E	MW535067
19.	2018	TNFxM19	Hills	Neiyamalai	Salem	Local	70.15^{ab}	11.78°N	78.47°E	MW535174

S. No	Year	Isolate code	Topo-graphy	Location	District	Cultivar	PDI	Geographical information		GenBank accession number
								Latitude	Longitude	
20.	2018	TNFxM20	Hills	Neyyamalai	Salem	Local	69.12^{bc}	11.78°N	78.47°E	MW494605
21.	2018	TNFxM21	Hills	Neiyamalai	Salem	Local	69.87^{ab}	11.78°N	78.47°E	MW498280
22.	2018	TNFxM22	Hills	Akkaraipati	Salem	Local	68.13^{bc}	11.47°N	78.06°E	MW504997
23.	2018	TNFxM23	Hills	Akkaraipati	Salem	Local	52.17^{f}	11.47°N	78.06°E	MW535244
24.	2018	TNFxM24	Plains	Valappadi	Salem	Local	34.15^{j}	11.39°N	78.23°E	MW504790
25.	2018	TNFxM25	Plains	Valappadi	Salem	Local	24.16^{l}	11.39°N	78.24°E	MW535295
26.	2018	TNFxM26	Hills	Karayankattupatti	Namakkal	Local	26.15^{l}	11.16°N	78.19°E	MW494589
27.	2018	TNFxM27	Hills	Vadakkadu	Namakkal	Local	39.34^{i}	11.23°N	78.20°E	MW497613
28.	2018	TNFxM28	Hills	Vadakkadu	Namakkal	Local	50.12^{fg}	11.23°N	78.20°E	MW535771
29.	2018	TNFxM29	Hills	Pagadupatu	Salem	Local	30.18^{k}	11.46°N	78.38°E	MW504990
30.	2018	TNFxM30	Hills	Adiyanur	Salem	Local	69.67^{b}	11.42°N	78.37°E	MW494316
31.	2018	TNFxM31	Hills	Kunnur (leaf)	Salem	Local	70.16^{ab}	11.43°N	78.37°E	MW535961
32.	2018	TNFxM32	Hills	Kunnur (sheath)	Salem	Local	11.24^{n}	11.43°N	78.37°E	MW496127

2 Means followed by the same letters were not significantly different from each other according to Tukey's test (P < 0.05). PDI: Percent
3 disease index

Table 2(on next page)

Table 2

Morphological and conidial characteristics of *M. grisea* isolates

1 **TABLE 2. Morphological and conidial characteristics of *M. grisea* isolates**

S. No	Isolates	Colour of vegetative growth	Colony texture	Conidial size (µm)		Conidial shape	Conidial colour
				Length	Width		
1.	TNFxM1	Slight greyish brown	Rough surface	22.64^l	9.12^{fg}	Pyriform	Hyaline to pale olive
2.	TNFxM2	Slight greyish brown	Smooth surface	22.80^l	6.88^{mn}	Pyriform	Hyaline to pale olive
3.	TNFxM3	Creamish white	Smooth surface	32.17^c	11.89^a	Pyriform	Hyaline to pale olive
4.	TNFxM4	Slight greyish brown	Smooth surface	25.63^{jk}	7.72^{ij}	Pyriform	Hyaline to pale olive
5.	TNFxM5	Greyish brown	Rough surface	26.84^{ij}	10.37^c	Pyriform	Hyaline to pale olive
6.	TNFxM6	Greyish brown	Rough surface	21.48^l	7.51^{jk}	Pyriform	Hyaline to pale olive
7.	TNFxM7	Greyish brown	Rough surface	37.76^a	7.12^{mn}	Pyriform	Hyaline to pale olive
8.	TNFxM8	Greyish brown	Rough surface	24.32^k	8.56^h	Pyriform	Hyaline to pale olive
9.	TNFxM9	Greyish brown	Rough surface	30.00^{de}	8.98^g	Pyriform	Hyaline to pale olive
10.	TNFxM10	Greyish brown	Rough surface	25.93^j	9.30^{ef}	Pyriform	Hyaline to pale olive
11.	TNFxM11	White	Smooth surface	27.44^{ghi}	9.68^{de}	Pyriform	Hyaline to pale olive
12.	TNFxM12	Greyish brown	Smooth surface	26.69^{ij}	7.94^i	Pyriform	Hyaline to pale olive
13.	TNFxM13	Greyish white	Smooth surface	28.63^{fg}	8.80^{gh}	Pyriform	Hyaline to pale olive
14.	TNFxM14	Greyish white	Smooth surface	28.41^{fgh}	8.43^h	Pyriform	Hyaline to pale olive
15.	TNFxM15	Greyish white	Smooth surface	28.52^{fg}	8.41^h	Pyriform	Hyaline to pale olive
16.	TNFxM16	White	Smooth surface	27.30^{hi}	8.43^h	Pyriform	hyaline to pale olive
17.	TNFxM17	Greyish brown	Rough surface	27.26^{hi}	7.47^{jk}	Pyriform	Hyaline to pale olive
18.	TNFxM18	Blackish white	Rough surface	26.77^{ij}	9.02^{fg}	Pyriform	Hyaline to pale olive
19.	TNFxM19	Greyish brown	Smooth surface	30.80^d	7.20^{km}	Pyriform	Hyaline to pale olive

20.	TNFxM20	Greyish white	Smooth surface	33.88^b	10.56^{bc}	Pyriform	Hyaline to pale olive
21.	TNFxM21	Greyish brown	Smooth surface	30.61^{de}	6.80^n	Pyriform	Hyaline to pale olive
22.	TNFxM22	Greyish brown	Smooth surface	24.83^k	9.87^d	Pyriform	Hyaline to pale olive
23.	TNFxM23	Greyish black	Smooth surface	20.06^m	9.60^d	Pyriform	Hyaline to pale olive
24.	TNFxM24	Greyish brown	Rough surface	27.12^{ghij}	9.06^{fg}	Pyriform	Hyaline to pale olive
25.	TNFxM25	Greyish brown	Rough surface	26.43^{ij}	9.80^d	Pyriform	Hyaline to pale olive
26.	TNFxM26	White	Smooth surface	25.68^{jk}	11.93^a	Pyriform	Hyaline to pale olive
27.	TNFxM27	Blackish white	Smooth surface	27.90^{fghi}	10.77^b	Pyriform	Hyaline to pale olive
28.	TNFxM28	Blackish white	Rough surface	28.44^{fgh}	9.67^{de}	Pyriform	Hyaline to pale olive
29.	TNFxM29	Greyish black	Rough surface	29.35^{ef}	8.98^{fg}	Pyriform	Hyaline to pale olive
30.	TNFxM30	White	Smooth surface	27.44^{ghi}	8.56^h	Pyriform	Hyaline to pale olive
31.	TNFxM31	Greyish brown	Smooth surface	28.41^{fgh}	8.43^h	Pyriform	Hyaline to pale olive
32.	TNFxM32	Greyish brown	Smooth surface	26.94^{hij}	7.94^i	Pyriform	Hyaline to pale olive

2 Values are mean of two observations. Means followed by the same letters were not significantly different from each other according to
3 Tukey's   test   (P   <   0.05).

4

Table 3(on next page)

TABLE 3.

Genetic analysis of *M. grisea* isolates with 29 SSR markers

1   **TABLE 3. Genetic analysis of *M. grisea* isolates with 29 SSR markers**

S. No.	Marker	Major allele frequency	Number of alleles	Gene diversity	Heterozygosity	PIC
1.	Pyrms 7-8	0.613	3.000	0.547	0.000	0.487
2.	Pyrms 15-16	0.500	4.000	0.633	0.000	0.570
3.	Pyrms 37-38	0.453	5.000	0.716	0.031	0.680
4.	Pyrms 39-40	0.453	3.000	0.639	0.031	0.565
5.	Pyrms 41-42	0.438	4.000	0.643	0.000	0.572
6.	Pyrms 43-44	0.688	4.000	0.484	0.000	0.443
7.	Pyrms 45-46	0.500	4.000	0.615	0.000	0.544
8.	Pyrms 47-48	0.813	4.000	0.328	0.000	0.313
9.	Pyrms 59-60	0.844	3.000	0.275	0.000	0.257
10.	Pyrms 61-62	0.438	4.000	0.650	0.000	0.585
11.	Pyrms 63-64	0.656	3.000	0.498	0.000	0.436
12.	Pyrms 67-68	0.875	2.000	0.219	0.000	0.195
13.	Pyrms 77-78	0.563	3.000	0.588	0.000	0.523
14.	Pyrms 81-82	0.438	3.000	0.619	0.000	0.539
15.	Pyrms 83-84	0.344	4.000	0.707	0.000	0.651
16.	Pyrms 87-88	0.500	4.000	0.635	0.000	0.574
17.	Pyrms 93-94	0.469	3.000	0.635	0.000	0.561
18.	Pyrms 99-100	0.453	3.000	0.625	0.031	0.546
19.	Pyrms 101-102	0.844	3.000	0.275	0.000	0.257
20.	Pyrms 107-108	0.875	2.000	0.219	0.000	0.195
21.	Pyrms 109-110	0.594	3.000	0.564	0.000	0.503
22.	Pyrms 125-126	0.438	4.000	0.627	0.000	0.552
23.	Pyrms 233-234	0.516	4.000	0.631	0.000	0.570
24.	Pyrms 319-320	0.656	4.000	0.521	0.000	0.479
25.	Pyrms 427-428	0.859	4.000	0.254	0.031	0.244
26.	Pyrms 453-454	0.594	5.000	0.602	0.094	0.569
27.	Pyrms 533-534	0.906	2.000	0.170	0.000	0.155
28.	Pyrms 607-608	0.844	3.000	0.275	0.000	0.257

29.	Pyrms 657-658	0.406	6.000	0.717	0.000	0.673
	Mean	0.605862	3.55	0.514172	0.007517	0.465345

2

3

Table 4(on next page)

TABLE 4.

Population structure group of *M. grisea* based on inferred ancestry values

1   **TABLE 4. Population structure group of *M. grisea* based on inferred ancestry values**

S. No	Isolates	Location (districts)	Topography	Inferred ancestry at K=2		Sub population
				Q1	Q2	
1.	TNFxM1	Tiruvanamalai	Plains	0.062	0.938	SP2
2.	TNFxM2	Dindigul	Plains	0.063	0.937	SP2
3.	TNFxM3	Dindigul	Plains	0.048	0.952	SP2
4.	TNFxM4	Dindigul	Plains	0.015	0.985	SP2
5.	TNFxM5	Dindigul	Plains	0.004	0.996	SP2
6.	TNFxM6	Virudhunagar	Plains	0.311	0.689	AD
7.	TNFxM7	Virudhunagar	Plains	0.144	0.856	SP2
8.	TNFxM8	Thoothukudi	Plains	0.060	0.940	SP2
9.	TNFxM9	Madurai	Plains	0.009	0.991	SP2
10.	TNFxM10	Dharmapuri	Plains	0.004	0.996	SP2
11.	TNFxM11	Vellore	Hills	0.017	0.983	SP2
12.	TNFxM12	Madurai	Plains	0.252	0.748	SP2
13.	TNFxM13	Erode	Hills	0.005	0.995	SP2
14.	TNFxM14	Erode	Hills	0.007	0.993	SP2
15.	TNFxM15	Salem	Hills	0.016	0.984	SP2
16.	TNFxM16	Salem	Hills	0.034	0.966	SP2
17.	TNFxM17	Salem	Hills	0.600	0.400	AD
18.	TNFxM18	Salem	Hills	0.374	0.626	AD
19.	TNFxM19	Salem	Hills	0.288	0.712	SP2
20.	TNFxM20	Salem	Hills	0.808	0.192	SP1
21.	TNFxM21	Salem	Hills	0.977	0.023	SP1
22.	TNFxM22	Salem	Hills	0.981	0.019	SP1
23.	TNFxM23	Salem	Hills	0.980	0.020	SP1
24.	TNFxM24	Salem	Plains	0.995	0.005	SP1
25.	TNFxM25	Salem	Plains	0.993	0.007	SP1
26.	TNFxM26	Namakkal	Hills	0.897	0.103	SP1
27.	TNFxM27	Namakkal	Hills	0.995	0.005	SP1

28.	TNFxM28	Namakkal	Hills	0.996	0.004	SP1
29.	TNFxM29	Salem	Hills	0.992	0.008	SP1
30.	TNFxM30	Salem	Hills	0.995	0.005	SP1
31.	TNFxM31	Salem	Hills	0.994	0.006	SP1
32.	TNFxM32	Salem	Hills	0.982	0.018	SP1

2